【Article】

Symmetry in Irregularity Generated by A Cellular Automaton of Earthquake

TAKAHASHI Koichi

Abstract It is shown that the coarse-graining reveals the quasi-periodicity and symmetric structure in irregularity generated in the deterministic cellular automaton model of earthquake. The structural symmetry reflects the symmetry in the dynamics and the boundary condition.

Keywords : self-organization, coarse-graining, rhythm, symmetry, earthquake

1. Introduction

The self-organization is the emergence of spatial patterns or temporal rhythms as are seen in viscous and traffic flows, the chemical and biological clocks etc. under steady supplies of resources or energies. Coexistences of rhythm and pattern are observed in many systems modeled by the method of cellular automaton (CA) (Wolfram 1994). Rhythm and pattern are manifested as a result of symmetry breaking.

Randomness in many degrees of freedom is expected to generally obscure the pattern and yield irregularity. This is also observed in the familiar models of earthquake. The point we should note is that earthquake is also a self-organized phenomenon at criticality (Bak et al. 1988). This has been well-acknowledged due to studies based on computer modeling by cellular automaton as well as two empirical laws : the Gutenberg-Richter-Ishimoto-Iida (GRII)'s scaling law concerning the frequency of seismic magnitudes (Gutenberg and Richter 1956 ; Ishimoto and Iida 1939) and the Omori's approximate scaling law (Omori 1894) for the temporal behavior of the frequency of aftershocks (Bak and Tang 1989).

The state of the CA is specified by the set of values associated to the cells. In the earthquake model, those values are the energies (or force. We utilize the terminology 'energy' because of its conceptual simplicity. See, e.g., Georgoudas et al. 2007.) loaded in the cells by the tectonic

stress. When the energy exceeds the critical value above which the cell ruptures, the cell's energy is transferred to its neighbors. In prevailing models, the cell whose energy is to be renewed is chosen randomly at each time step. This process is also responsible for the irregularity in the outcome of such kind of models (Bak and Tang 1989, Ito and Matsuzaki 1990, Barriere and Turcotte 1994) .

What happens if the sandpile-like earthquake model is modified to a deterministic one ? (A deterministic CA model with continuous variables has been analyzed by Nakanishi (1991).) Sammis and Smith (1999) found that rhythm emerges if initial energies are randomly distributed between zero and the critical value and the efficiency of the energy transfer is less than one. The 'period' reflects the time that a cell requires from reloading to redistribution in triggering a large event.

What if the initial energies are distributed in a narrow band? This question has been partially answered by Takahashi (2011). There, the same amount of energy is supplied to all the cells with a constant rate. Again, the two scaling laws, the GRII's law and the Omori's law were reproduced. It is noteworthy that, at the same time, the signs of the quasi-periodicity and the fractal-like spatial pattern were observed. This model can accommodate the static periods. We would like to elucidate these features of the self-organization in the deterministic model more quantitatively.

The purpose of this paper is to analyze the CA model proposed in Takahashi (2011) in detail and elaborate its intriguing nature : rhythm and symmetry in irregularity originated from randomness. By randomness, we mean that the values of the cells in the initial state are randomly distributed and the subsequent time evolution of the state involves irregularity that is discriminated from chaos in continuous systems. Specifically, a stress is put on the significance of coarse-graining (or rounding) of the cell's energy in observing submerged patterns. In the followings, the attention is put rather on the numerical and algorithmic properties of the model than on the correspondence to physical reality.

2. Model

Our CA consists of $L \times L$ square lattice of cells, each of which is specified by the coordinate suffixes (i, j). The state of a cell (i, j) is specified by its energy $E_{i,j}$. At every discrete time t, all the cells are subjected to the accumulation of energy

$$E_{i,j} \to E_{i,j} + \varepsilon. \tag{1}$$

as long as the energy does not exceed the critical value, 4.

The cell whose energy is equal to or exceeds 4 is called *critical*. If $E_{i,j}$ is critical, its energy is

redistributed to the nearest neighbors at the next time step according to the rule

$$E_{i,j} \to E_{i,j} - 4, \tag{2a}$$

$$E_{i\pm1,j} \to E_{i\pm1,j} + 1, \tag{2b}$$

$$E_{i,j\pm1} \to E_{i,j\pm1} + 1. \tag{2c}$$

In (2b) and (2c), the peripheral cells are supposed to release some part, i.e., either 1/4 or 1/2 depending on their locations, of their energies to the outer surroundings. Note that the dynamics and the boundary have the C_{4v} symmetry of point group.

The constant supply of energy (1), which is halted while the above energy redistribution is taking place, is done when no critical cell is present. The revisions of energies (2) are executed on computer in a spatially definite order that is kept unchanged throughout the calculations. The system is deterministic and differs from the familiar CA model (e.g., Bak and Tang 1989), in which the cell to be revised is chosen randomly at each time step. The cell releasing its energy by (2a) is called *active*. When there is no active cell, the energy of each cell steadily increases. Such cells are called *static*.

3. Rhythm

The temporal irregularity during the process of the energy redistribution is clearly observed by the behavior of the quantity

$$\Delta_{i,j}(t) \equiv E_{i,j}(t) - E_{i,j}(t-1) - \varepsilon. \tag{3}$$

By deleting the effect of the constant energy supply (1), $\Delta_{i,j}(t)$ measures the degree of the effect of the dynamics (2). It is nonzero when some cell is active at $t-1$ and the neighboring cell (i, j) is affected at the next time t by the subsequent energy redistribution. Shown in Fig. 1 are the temporal behaviors of $E_{21,21}(t)$ and $\Delta_{21,21}(t)$ of the system with the size L=40, ε=0.005. The cell (21, 21) is one of the four cells that locate at the center of the lattice. The initial condition was set randomly by

$$E_{i,j}(0) = 4 - r, \tag{4}$$

where r is a uniform random number in [0, a] with $0 \le a \le 4$. In the following numerical calculations, we set a=0.5. $\Delta_{21,21}$ changes randomly between positive and negative values. In *static* periods, $E_{21,21}$ linearly increases while $\Delta_{21,21}$ is zero.

The time series is random but the transition of the state of the cell tends to occur in adjacent

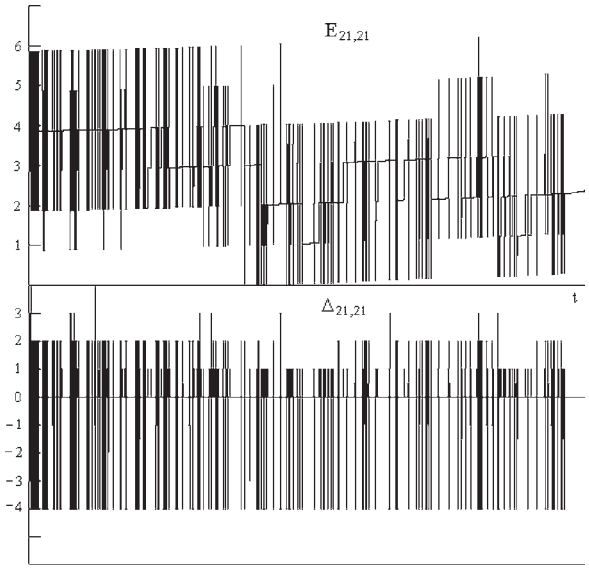

Fig. 1　An example of the temporal behaviors of $E_{ij}(t)$ and $\Delta_{ij}(t)$ from t=0 to 7,692 in a system with L=40, ε= 0.005, r=0.5.

times.　This tendency is also manifested by examining the Fourier expansion of $\Delta_{21,21}$:

$$\Delta_{21,21}(t) = \frac{1}{\sqrt{T}} \sum_{j=0}^{T-1} v_j e^{2\pi i(t/T)j}. \tag{5}$$

The behavior of $|v_j|$ is given in Fig. 2.　We note that the amplitude is more dominant for higher frequency as $|v_j| \propto j$.

In short, for each active period, it is hard to extract any regularity in the change of a single cell-

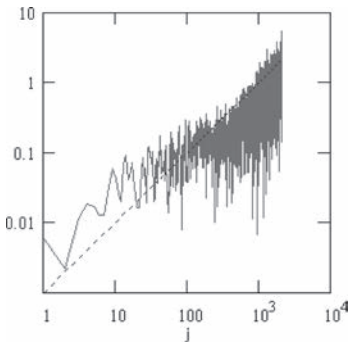

Fig. 2　Spectrum of the absolute values of the Fourier components of the time series shown in Fig. 1.　Dotted line which denotes j/1,000 is also shown as comparison.

state. Similar result has been obtained by the stochastic CA model of earthquake (Bak and Tang 1989 ; Ito and Matsuzaki 1990). Their result was that the events of energy redistribution take place randomly and there seemed to be no apparent periodicity. Bak and Tang (1989) then concluded that earthquake is unpredictable.

Our deterministic model and the stochastic model have two things in common. One is that the rate of the energy supply is constant. The other is that the energy flows out from the boundary of the finite lattice of cells. These features, an idealization of real earthquakes at faults with tectonic origin, allow us to expect to define the averages of the period. We utilize the terminology quasi-periodicity for the existence of this average with not large a dispersion. The indication of the quasi-periodicity in CA model has been noticed by Takahashi (2011) in the deterministic model.

Since the energy governs the dynamics, one of the appropriate quantities for extraction of the temporal behavior in the system may be the total energy. Therefore, we define the average energy by

$$< E > = \frac{1}{L^2} \sum_{i,j} E_{i,j} \tag{6}$$

and see its time dependence. The result is shown in Fig.3, where now the behavior of $E_{1,1}$ is also shown.

The system was initially prepared with relatively higher energy. $< E >$ gradually decreases in the active period of length T_a, and then, in the subsequent static period of length T_s, increases linearly. The decreases of $< E >$ in active periods are also approximately linear except for in the first one. In Fig.3, the quasi-periodicity of $< E >$ is obvious, as compared with $E_{1,1}$ shown in the same figure. The cell (1,1) locates at one of the corners of the lattice and, like the cell (21,21), exhibits no clear quasi-periodicity. This indicates that it will be difficult to grasp the pattern the system generates as a whole if we always focus our attentions to the individual cell's state.

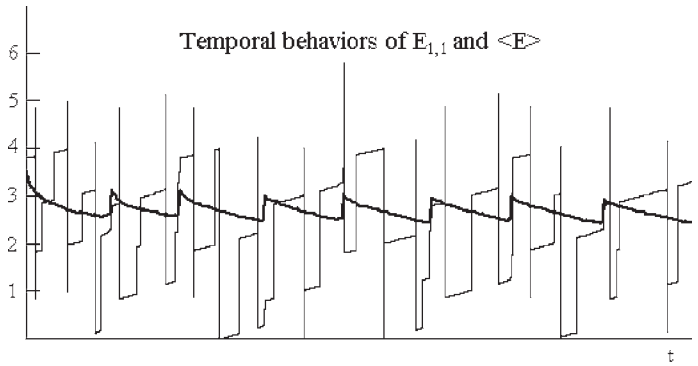

Fig. 3 Temporal behavior of $<E>$ (thick line) and $E_{1,1}$ (thin line) in $0 \leq t \leq 57,618$ for L=40.

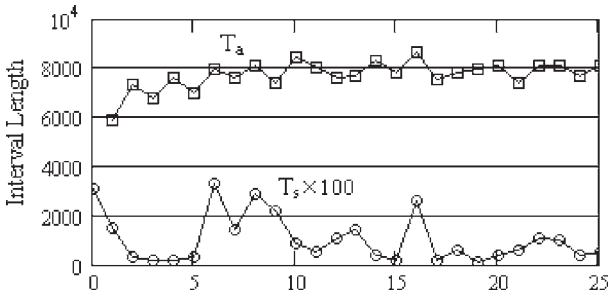

Fig. 4　Interval length of the active period T_a and the static period T_s extracted from the result shown in Fig. 3.

Stochasticity will tend to obscure the quasi-periodicity.　Ito and Matsuzaki introduced probability for the energy redistribution (2) to take place (Ito and Matsuzaki 1990).　The temporal behavior of $< E >$ they found has in fact poor quasi-periodicity even for a very small probability of energy redistribution.

We extracted in our model the duration lengths of each active and static periods.　The calculations were performed till the system experiences twenty five quasi-periods.　The result is shown in Fig. 4 in the order of appearance.

By discarding the first nine transient data, the lengths of the quasi-period, $T=T_a+T_s$, are found to be in the range of 7,956±314.　T is expected to be approximately proportional to L^2.

The simple quasi-periodic behavior the system exhibits as a whole is remarkable, considering the randomness of the state of individual cells.　We may eventually anticipate some quasi-periodicity since the energy input to the system is steady and the rule of energy release is fixed as (2).　Actually, the fluctuation of periods is small.　On the other hand, determining a priori the length of each period from the rule (1) and (2) seems difficult.

Generally, the energy of the individual cell varies quite irregularly, but the average $< E >$ does not.　Taking average is a kind of coarse-graining.　(Coarse-graining is the procedure designed to find a representative value of the system's physical quantity from its local values.) Thus, we expect that the temporal pattern observed in $< E >$ indicates the importance of coarse-graining to extract a global pattern resulted from self-organization.

4.　Symmetry

We spatially 'coarse-grain' the system by grading the energy of each cell and take a look at the pattern of the graded energies.　Let us classify the energy into five categories : (0) $0 \leq E < 1$, (1) $1 \leq E < 2$,

(2) $2 \leq E < 3$, (3) $3 \leq E < 4$, (4) $4 \leq E$. Namely, our 'coarse-graining' is nothing but the rounding of E for the categories (0)〜(3). Here and in the followings, the width of the coarse-graining is set to be unity. Then, we observe an interesting phenomenon to take place at the beginning of each static period. In the previous work, we saw that, by the coarse-graining of the energies, the system passes through a symmetric state at the onset of the static phase (Fig. 2 in Takahashi 2011). This kind of state in the system of L=40, together with the preceding three typical states, is depicted in Fig. 5, where the five energy grades are visualized by five grey scales.

The first active period ceases at t=7,359. The last state at t=7,360 depicted in Fig. 5 is the initial one in the static period and possesses C_{4v} symmetry. The emergence of exactly symmetric state was not expected because the initial state of each cell has been set randomly and this relative randomness among cells is kept unchanged throughout the time evolution due to the symmetric rules (1) and (2). In fact, the characteristic patterns formed by the distribution of the coarse-grained energies are random in the active period as is seen in Fig. 5.

In general, for our choice of parameter values, a symmetric pattern emerges when any active period ceases and then the static period starts. In other words, the system passes through the symmetric

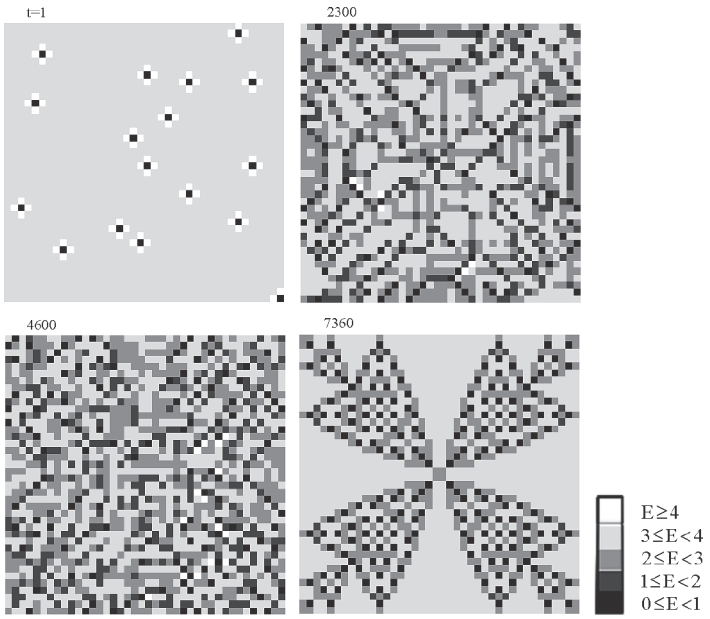

Fig. 5 Energetically coarse-grained states in the first active period generated from a specific initial condition. The times are t=1 (top left), 2,300 (top right), 4,600 (bottom left) and 7,360 (bottom right). In this example, the active period continues from t=1 to 7,359, and the static period begins at t=7,360. Five grey scales designate the energy ranges denoted in the figure, i.e., black : $0 \leq E < 1$, dark gray : $1 \leq E < 2$, medium gray : $2 \leq E < 3$, light gray : $3 \leq E < 4$, white : $E \geq 4$.

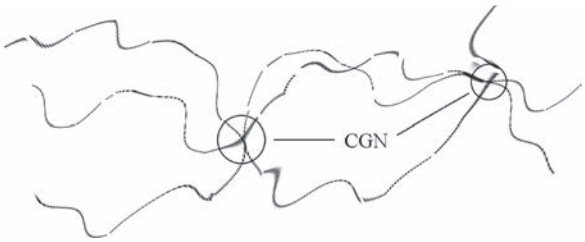

Fig. 6　Schematic representation of CGNs.　Here, three trajectories are going in and out a CGN.　Distinctions of trajectories are reflections of differences in the initial conditions and/or the algorithms adopted in computations.

coarse-grained state shown in Fig.5 irrespective of randomness of the initial state and irregularity of motions in the precedent first active period.　In this sense, this symmetric pattern is stable.　This implies that the symmetric state depicted in Fig.5 is a kind of node which the trajectories in the space of states pass through.　We shall call this type of state the coarse-grained node (CGN).　See Fig. 6.

The first sixteen coarse-grained states at the onsets of the static phase are collected in Fig. 7 in temporal order.　They noteworthily possess exact C_{4v} symmetry.　Small changes in the initial state do not change these patterns as well as the order of emergences, although the evolutions in the active periods are quite irregular and are dependent on the initial condition.　In this sense, the states shown in Fig. 7 are CGNs defined above.　We may say that, when energy is coarse-grained, memory of initial condition is forgotten in the early stage of the static periods and then recalled during the active periods.

Self-similarity is essential for scaling laws to hold.　One can get the scaling laws even only counting the overlap of two fractal patterns in relative motion (Chakrabarti and Stinchcombe 1999, Pradhan et al 2003, Bhattacharaya et al 2006).　From this view point, it is also notable that glimpses of self-similarity of the spatial pattern, which is expected from the GRII's scaling law, are observed in 01～03 in Fig. 7.　These self-similar patterns are not given by an external condition (Barriere and Turcotte 1994) but are dynamically generated.　Larger lattice sizes will be able to manifest this feature more clearly, as is shown in Fig. 8.

Now we shall give a proof of the existence of C_{4v}-invariant CGNs in an arbitrary square lattice.　The proof follows two steps.

Lemma

In case r is a fixed number and $E_{i,j}(0)$ in (4) are independent of i and j, the static states are C_{4v}-invariant and algorithm-independent.

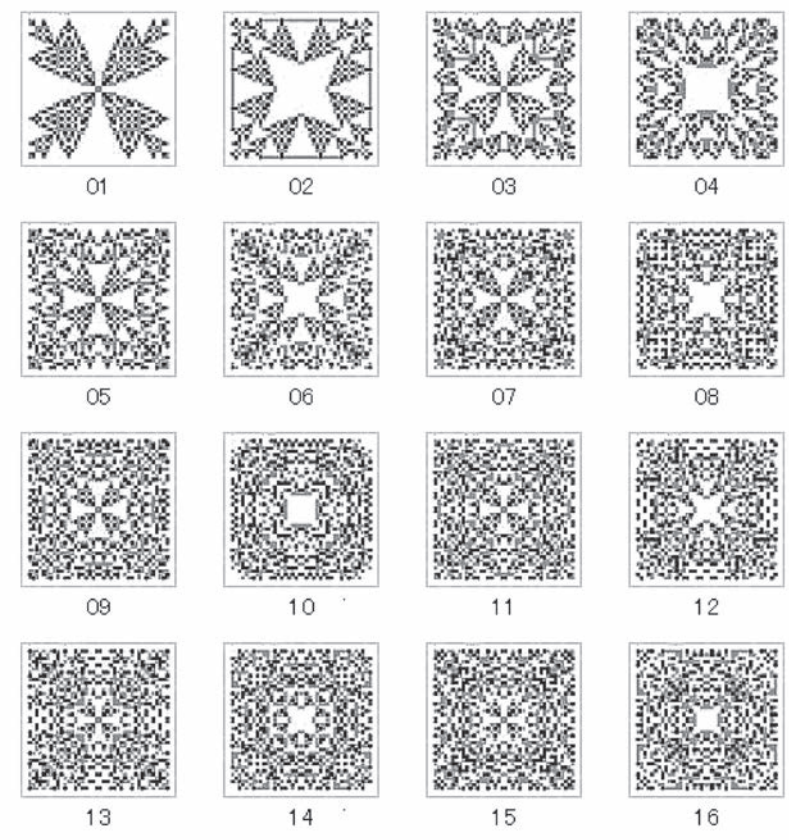

Fig. 7 First sixteen CGNs in the temporal order. L=40. The values of the parameters are same as the ones in Fig. 5.

Proof

All cells initially have the same energy given by $E_{i,j}(0)=4-r$. The initial state is therefore C_{4v}-symmetric. The state remains C_{4v}-symmetric since the energy of each cell is increased by the same amount ε until the cells become critical. All the cells become critical simultaneously and release the same amount of energy C_{4v}-symmetrically, i.e., to their Neumann neighbors.

If the computational algorithm has been constructed so as for all the cells to release their energies *simultaneously*, then the system's state is C_{4v}-symmetric at any computational step. Consequently, the CGNs are also C_{4v}-symmetric.

If the computational algorithm has been constructed so as for the cells to release their energies *not* simultaneously (e.g., sequentially from left to right and from bottom to top), then C_{4v} is generally broken at every computational step. However, this kind of change in the algorithm brings about a mere change of the order of the additions and subtractions in the calculations associated to the energy redis-

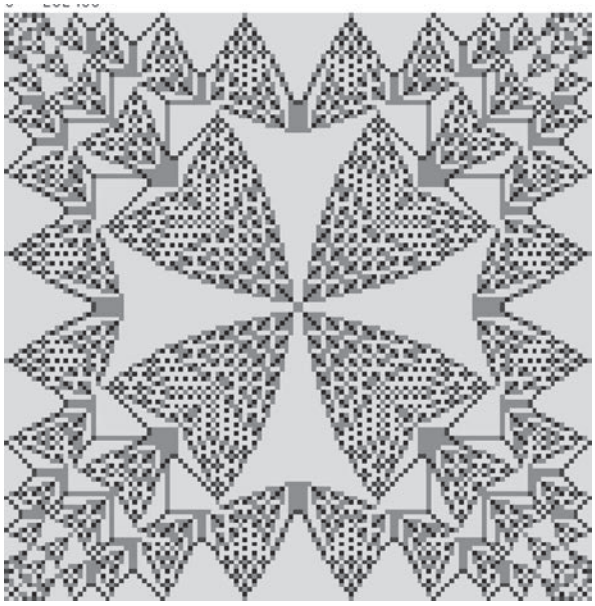

Fig. 8　The first CGN in the system with the size 128×128.　The self-similarity is more clearly observed than the case of smaller lattice.　The values of the parameters other than L are same as the ones in Fig. 5.

tribution (2).　Addition and subtraction commute.　Therefore, after all of the cells were revised, the final state of the system coincides with the one that resulted by the simultaneous-change-algorithm.　Since the energies are supplied in C_{4v}-invariant way, the states in the following static period are also C_{4v}-symmetric.　■

Theorem

For a given square lattice, there exist C_{4v}-symmetric CGNs for the initial condition given by (4).

Proof

Case 1.　$a \leq \varepsilon < 1$.

a is the variance of the initial values that is smaller than unity, which means that all cells are in the same category of coarse-graining.　The energy ε is supplied to each cell at $t=1$.　Since $a \leq \varepsilon$, the energies of all cells exceeds 4 simultaneously at $t=1$ and are revised simultaneously, too, according to (2).　In this case, the coarse-grained system behaves in a same way as that of $r=0$ and the argumentation given in the proof of the lemma is applicable.　The state after the revisions of all the cells completed is necessarily C_{4v}-symmetric.

Case 2.　$\varepsilon \leq a < 1$.

If the energy supplied to each cell were a then all the cells would become critical simultaneously and transferred the energy of equal amount 1 to the neighboring four cells.　Following the argumen-

tation in Case 1, the resultant energy distribution would again have C_{4v}-symmetry when the energies were coarse-grained with the width of 1.

Actually, the energy ε supplied to each cell at each time step is smaller than a. Then the sufficient amount of energy-supply to render the system active is eventually achieved after the supplies of unit energy ε were done $[a/\varepsilon]+1$ times, where [ ] is the Gauss symbol. In the course of this temporal evolution, the system undergoes changes through only additions and subtractions of energies to the cells. Any such procedures do not alter the final result because additions and subtractions commute. Therefore, the actual trajectory also passes the same C_{4v}-symmetric CGNs as the system with $\varepsilon > a$ generates. ■

The long range correlations in the CGNs shown in Figs. 7 and 8 are manifested as the symmetries that are due to the symmetry of the dynamics and the boundary condition. There are four symmetry axes and three rotations in C_{4v}. How much degree does the symmetry break or restore during the course of the time evolution ? In order to answer this question quantitatively, we introduce the symmetry breaking parameters B_M and B_R by

$$B_M = \frac{1}{L}\sqrt{\sum_{i,j}([\mathfrak{M}\,E]_{i,j} - [E]_{i,j})^2}, \tag{7a}$$

$$B_R = \frac{1}{L}\sqrt{\sum_{i,j}([\mathfrak{R}\,E]_{i,j} - [E]_{i,j})^2}. \tag{7b}$$

Here $\mathfrak{M}$ denotes one of the four mirror reflections that keep the interaction (2) invariant. Similarly, $\mathfrak{R}$ denotes one of the three rotations. $\mathfrak{M}\,E$ and $\mathfrak{R}\,E$ are the new arrangements of energies after the operation $\mathfrak{M}$ and $\mathfrak{R}$ were applied. $[E]$ is the coarse grained configuration defined by $[E]_{i,j}=[E_{i,j}]$. B_M and B_R are the Hamming distances divided by L between the configurations before and after operating $\mathfrak{M}$ and $\mathfrak{R}$ on the state. If C_{4v} is exact, B_M and B_R both vanishes. These will be equal to 2 if cell states are not correlated and randomly take value from 0 to 4 with equal probability. Taking $\mathfrak{M}$ as the reflection about the vertical-axis passing the center and $\mathfrak{R}$ as the $\pi/2$ rotation about the center of the lattice, we calculated numerically the temporal variations of B_M and B_R. The result is shown in Fig. 9.

Frequently fluctuating around the averages, B_M and B_R take approximately constant values between 1 and 2 in active periods. At the onset of the ensuing static periods, B_M and B_R becomes exactly zero. In other words, the exact C_{4v} is quasi-periodically recovered. The above theorem tells us nothing about how frequently the system visits the symmetric CGN. The quasi-periodicity is rather surprising considering the randomness in the active periods.

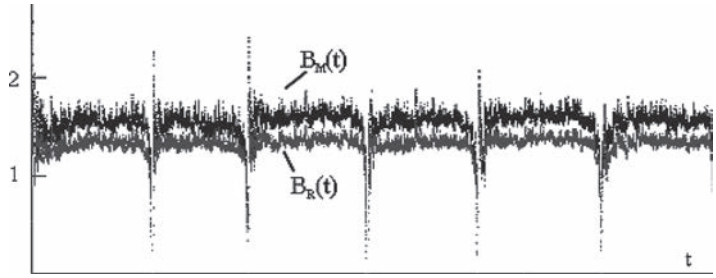

Fig. 9　Temporal behaviors of the symmetry breaking parameters B_M and B_R for r=0.5.　Time is from zero to 42,029.

5.　Not Chaos

Is the irregular behavior of our deterministic system chaotic?　Deterministic chaos requires at least two features :　sensitivity on the control parameters, and sensitivity on the initial conditions.　In this section, we focus our attention to the latter.

The sensitivity on the initial condition will be measured by the rapidity of separation of two orbits whose initial condition differs only slightly.　We define the normalized distance $d(t)$ at time t by the hamming distance between two states at time t on different orbits divided by L.　Thus

$$d(t)=\frac{1}{L}\sqrt{\sum_{i,j=1}^{L}\left(E_{i,j}^{(a)}(t)-E_{i,j}^{(b)}(t)\right)^2}, \tag{8}$$

where (a) and (b) denote the states.　For simplicity, the two initial states are randomly prepared so that $\Delta^{(a,b)}(0)\equiv E_{i,j}^{(b)}(0)-E_{i,j}^{(a)}(0)$ are independent of the lattice cites.　We investigate two cases :　$\Delta^{(a,b)}(0)=0.0001$ (A) and 0.0002 (B).　The result is shown in Fig. 10.

The behaviors of $d(t)$ and $d(t)\equiv d(t+1)-d(t)$ show no rapid separation of orbits.　Although not shown here, various initial conditions are examined with the same conclusion.

The marked aspect of our system is the presence of the stable CGNs which orbits pass through.　By 'stable' we mean that CGN is not changed by a small change of initial condition.　Truly chaotic systems, however, do not behave in this way.　As an example, let us recall the logistic map $x_{t+1}=4x_t(1-x_t)$ that exhibits chaos.　If we coarse-grain the value of the variable by the correspondences（0, 0.5）→0 and (0.5, 1)→1, then we have any series of 0 and 1 by varying the initial value.　The absence of the CGNs in the logistic map is due to the positive Lyapunov index.

In the above logistic map, when x_t is small, the locally exponential separation of two orbits is expected from the linearized equation $dx_t/dt\sim 3x_t$ with continuous time.　In other words, one of the two aspects of chaos, stretch and folding, is confirmed to be present.

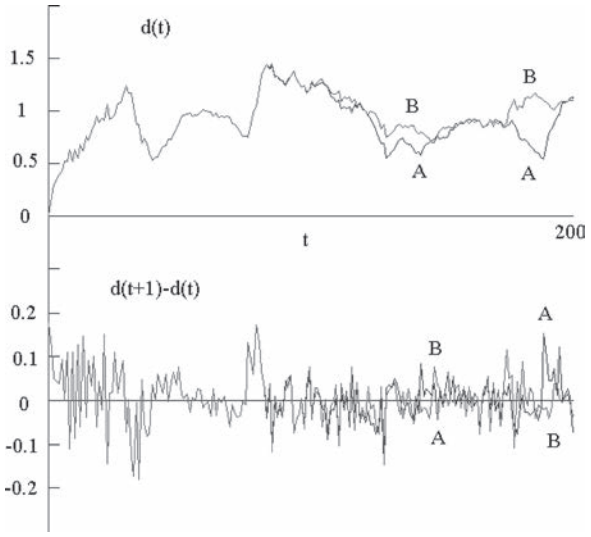

Fig. 10 Time-dependences of the Hamming distance (upper graphs) and of the time-differences of the hamming distance (lower graphs) of two close orbits for two cases A and B. In case A, the initial value of each cell of one orbit is increased by 0.0001 from the corresponding value for the other orbit, while, in case B, the increment is 0.0002. The lattice size is 25×25.

In the present problem, we may turn the variables continuous by rewriting the equation of motion as

$$\dot{E}(\boldsymbol{r}) = -e_0\,\theta(E(\boldsymbol{r})-E_c)+\sum_{\Delta\boldsymbol{r}} e_1\,\theta(E(\boldsymbol{r}+\Delta\boldsymbol{r})-E_c). \tag{9}$$

Here $\Delta\boldsymbol{r}$'s are the position vectors of the neighboring sites. θ is the Heaviside function. The above equation implies that the site at $\boldsymbol{r}$ loses energy when the energy exceeds the critical value, while it gains energy when surrounding sites have energies greater than the critical one. The local energy conservation poses a constraint on e_0 and e_1 :

$$e_0 = \sum_{\Delta\boldsymbol{r}} e_1. \tag{10}$$

We assume $E(\boldsymbol{r})$ and its derivatives are sufficiently small. Furthermore, we replace the function θ by some positive differentiable function, Θ, that behaves as $\Theta(x)\to0$ for $x\to-\infty$, $\Theta(x)\to1$ for $x\to+\infty$ and $\Theta(x)+\Theta(-x)=1$. Performing Taylor expansion of E and Θ, and keeping up to the terms linear in E, we have

$$\dot{E}(\boldsymbol{r}) = -e_0\,\Theta(E-E_c)+\sum_{\Delta\boldsymbol{r}} e_1\,\Theta(E-E_c)+\sum_{\Delta\boldsymbol{r}} e_1\,\Theta'(E-E_c)(\nabla E\cdot\Delta\boldsymbol{r}+1/2\,\nabla\nabla E\cdot\Delta\boldsymbol{r}\,\Delta\boldsymbol{r}). \tag{11}$$

Let us assume isotropy of the solution. Then, the liner and cross terms of $\Delta\boldsymbol{r}$ are dropped. We finally have

$$\dot{E}(\boldsymbol{r}) = \frac{1}{2}\Big(\sum_{\Delta \boldsymbol{r}} e_1(\Delta \boldsymbol{r})^2\Big)\Theta'(E-E_c)\nabla^2 E, \tag{12}$$

where a use has been made of (10). If $\Theta'(E-E_c)$ on the r.h.s. is replaced by a constant, (12) is noting but the diffusion equation, which allows only locally decaying solutions.

We conclude that the CA of earthquake does not produce chaos originated from stretch and folding. Instead, the large degrees of freedom are responsible for the irregularity we have observed in this paper.

6. Summary

We showed that, irrespective of the dominance of irregularity during the course of time evolution, the deterministic CA model presented in this article exhibits self-organization as the emergence of the temporal rhythm and symmetric spatial structures simultaneously. This spatio-temporal structure is conceivable only when the energy is coarse-grained in the sense mentioned so far. The origin of the symmetry is the symmetry in the dynamics and the boundary condition, while the irregularity is attributed to the randomness of the initial condition that is possible under sufficiently many degrees of freedom.

A simple or symmetric initial state does not always lead to a regular motion. Rather, it is frequently observed that the temporal behavior of the individual cell-state is quite irregular irrespective of the choice of the initial state. One may say that our system is macroscopically homoplex and microscopically autoplex (Wolfram 1994).

Some interesting questions arise. What is the basin of attraction to CGNs ? How does stochasticity in dynamics obstruct the organization ? These are left as open problems for future studies.

References

Bak P and Tang C 1989 *J. Geo. Res*. **94** 15635.
Bak P, Tang C and Wiesefeld S 1988 *Phys. Rev*. **A 38** 364.
Barriere B and Turcotte D L 1994 *Phys. Rev.* **E49** 1151.
Bhatacharaya P, Chakrabarti B K and Kamal 2011 *J. Phys.* : *Conference Ser.* **319** 012004
Chakrabarti B K and Stinchcombe R B 1999 *Physica* **A 270** 27.
Georgoudas I G, Sirakoulis G.Ch. and Andreadis I 2007 *Mathematical and Computer Modelling* **46** 124.
Gutenberg B and Richter C F 1956 *Ann. Geofis*. **9** 1.
Ishimoto I and Iida K 1939 http://hdl.handle.net/2261/1044.
Ito K and Matsuzaki M 1990 *J. Geo. Res*. **95** 6853.
Nakanishi H 1991 *Phys. Rev.* **E43** 6613.

Omori F 1894 *J. Coll. Sci. Imp. Univ. Tokyo* **7** 111.
Pradhan1 S, Chakrabarti B K, Ray P and Dey M K 2003 *Phys. Scr* **77** 106a00077.
Sammis C G‐ and Smith S W 1999 *Pure and Appl. Geophys*. **155** 307.
Steacy S J and McCloskey J 1998 *Geophys. J. Int.* **133** F11.
Takahashi K 2011 *Faculty of Liberal Arts Review*, *Tohoku Gakuin Univ*. **160**.
http://www.tohoku‐gakuin.ac.jp/gakujutu/kyoyo_160/index.html/
Wolfram S 1994 *Cellular Automata and Complexity* (Addison‐Wesley, Massachusetts)